

THE AXIAL INJECTION SYSTEM AT THE K.V.I.

W.K. van Asselt, O.C. Dermois, A.G. Drentje and H.W. Schreuder.

Kernfysisch Versneller Instituut, Zernikelaan 25, 9747 AA Groningen, the Netherlands.

**Abstract.** - Heavy ion beams for the KVI cyclotron will be produced in an ECR type ion source, with emphasis on highly charged ions, and in a PIG source set-up, to be used with presently available sources. The properties of the beam transport lines are described. A periodic focussing structure with permanent magnets has been adopted for the vertical beam line. The characteristics of this system are discussed; special attention is given to beam behaviour and technical realisation. The influence of the cyclotron stray field will be reduced by means of two arrays of three iron plates on top of the yoke. A hyperboloidal inflector will guide the beam excentrically into the median plane; the centering will be realized within approximately 10 turns by means of field bumps. The properties of this central region are discussed.

**Introduction.** - The axial injection project, outlined at the previous conference <sup>1)</sup> incorporates the construction of an external source set up, a horizontal beam line in the source area, a vertical beam line with a periodic focussing structure, and an inflector in the cyclotron centre. The source set up is a large magnet in which the presently available internal source can operate. In addition to this an ECR-type ion source -Micro Mafios- <sup>2)</sup> has been ordered, which is being constructed at CEN-G (R. Geller). This implies that heavy ions of higher charge states will become available; it is expected that maximum beam energies for oxygen, neon, argon and krypton will be 40, 32, 16 and 5 MeV/amu respectively.

**Horizontal beam line.** - The layout of the source area is shown in fig. 1. Beams from the ECR source are charge state analysed by a 110° magnet (with entrance and exit slits of 10 mm width) and transported by means of two quadrupole triplets to a 90° bending magnet, see fig. 2. Two cylindrical magnetic adaptor lenses will match the beam phase space (max. 700 mm mrad) to the acceptance of the periodic focussing structure, described below.

The analyser can separate ion beams with mass-to-charge ratio differences of 1.2% or more, which is sufficient in most cases. If needed, e.g. for separation of  $^{131}\text{Xe}^{18+}$  and  $^{132}\text{Xe}^{18+}$ , the slit widths have to be decreased, of course leading to reduction of beam current. However, once the cyclotron is tuned to the desired beam, the resolving power of the cyclotron is much larger so that the analyser slits can be opened to normal. This is of course the only way to separate ions like  $^{12}\text{C}^{6+}$  and  $^{16}\text{O}^{8+}$ .

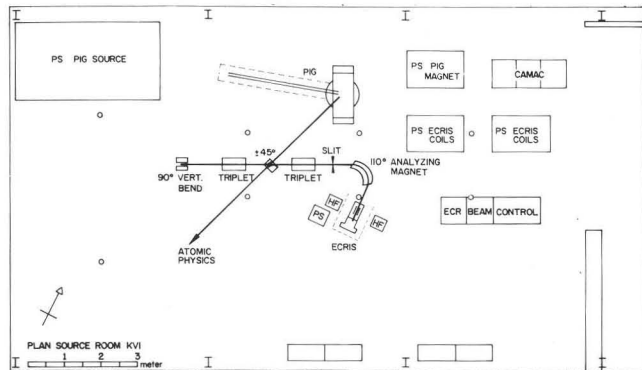


Fig. 1 : Layout of the source area. The beam lines are approximately 9 meter above the cyclotron median plane.

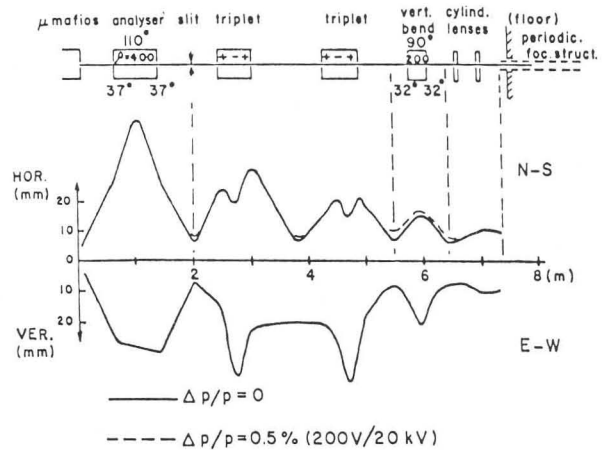


Fig. 2 : Envelopes calculated for a 700 mm mrad beam from the ECR source with the same rigidity as 20 kV deuterons. The location of some beam diagnostic tools are indicated by vertical dashed lines

N-S (from HOR.)

E-W (from VERT.)

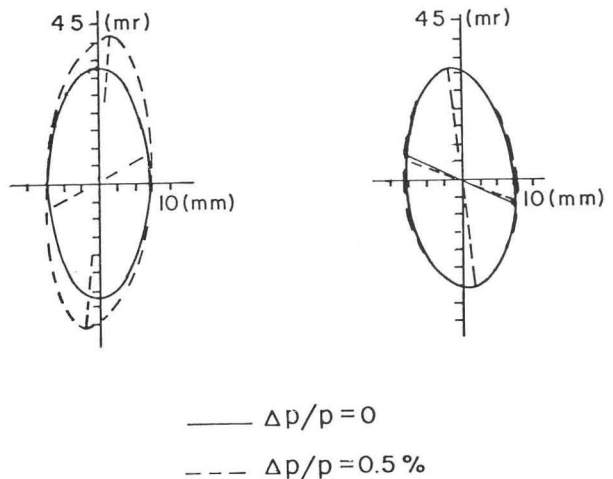


Fig. 3 : Phase space ellipses at the position of the exit waist below the 90° bending magnet. This magnet converts the horizontal plane, in which the charge state analysis occurs, into the N-S plane and the non-dispersive vertical plane into the E-S direction

The momentum dispersion in the vertical beam line, produced by the vertical bending magnet is relatively small, since a small radius magnet is used. If one allows a momentum spread in the primary beam as large as 0.5%, the phase space in the horizontal plane will increase because of the analyser, which will appear after the 90° vertical bend as a 30% enlarged area; the increase in the transverse direction due to the dispersion of the 90° magnet will be not more than 5% (see fig. 3). Therefore it was decided not to install a more complicated and expensive achromatic vertical bending system.

In view of interest shown by atomic physicists, space has been created for their experiments with beams of both ion sources. The analyser handles all possible beams at 5 kV, except very rigid ions like Xe<sup>1+</sup>.

The periodic focussing structure, - The properties of this structure are discussed in 3) and more extensively in 4). Here the emphasis will be on the technical aspects and beam behaviour.

Fig. 4 shows the arrangement of focussing elements around the beampipe. The small diameter rings are made of anisotropic ferrite and axially magnetized. They are separated by radially magnetized isotropic ferrite rings. Two halves of radial- and five axially magnetized rings form one system element. This length has been chosen to minimize the aberrations. The field direction is reversed in two adjacent elements. In such a system the particle trajectory can be described by the Mathieu-Hill equation but in this case, due to the long period of the trajectory, equally well by a succession of thin lenses in each of which the following equation holds:

$$\frac{d^2r}{dz^2} + \frac{1}{8} \frac{qe}{m} \frac{B^2}{V} r = 0 \quad r = \text{radial distance, } z = \text{axial distance, } V = \text{acceleration voltage.}$$

One element of the structure behaves as a thin lens with lens strength:

$$k = \frac{1}{8} \frac{qe}{m} \frac{1}{V} \int_0^{\lambda} B^2 dz \quad \lambda = \text{length of one element.}$$

In phase space,  $rr'$ , particles follow the so called "eigenellipse". Here the eigenellipse is always upright with axis ratio  $\alpha = \frac{r_{\max}}{r_{\min}} \approx \left(\frac{k}{\lambda}\right)^{\frac{1}{2}}$  and step angle  $\phi \approx (k\lambda)^{\frac{1}{2}}$ . For 20 keV deuterons the following numbers hold:  $Bp = 2.88 \cdot 10^{-2} \text{ Tm}$ ;  $k = 0.46 \text{ m}^{-1}$ ;  $\alpha = 2.52 \text{ m}^{-1}$ ;  $\phi = 10.6^\circ$ ; trajectory period  $p = 2.48 \text{ m}$ .

The beam will be ideally matched to the system if at the entrance the circumference of the phase-space area is an eigenellipse. In this case the beam leaves the system as it comes in and has the same diameter everywhere, with a small ripple having a period of two elements. The axis ratio  $\alpha$  is inversely proportional with  $(V)^{\frac{1}{2}}$  so as function of energy the phase space area has a variable geometry. An important property is that the scaling factor for  $\alpha$  is the same as for the beam emittance when for different energies the same source is used. In our system a 600 mm mrad 20 keV deuteron beam has a diameter of 17.4 mm and a 2 keV or 200 keV beam would have the same diameter. Given the fact that source emittances are normally smaller than the given value it means that the system is equally well suited for lower and for higher energies.

The aberrations and the influence of space charge are treated in 4). Fig. 5 shows the distorted eigenellipse, or phase-space boundary, for a 600 mm mrad beam of 20 keV deuterons after two trajectory periods. The third period is shown together with the boundary at the entrance. The increase in area is about 8 % but it contains less than 4 % of the particles assuming a homogeneous density distribution at the entrance. This is due to the quadratic nature of the

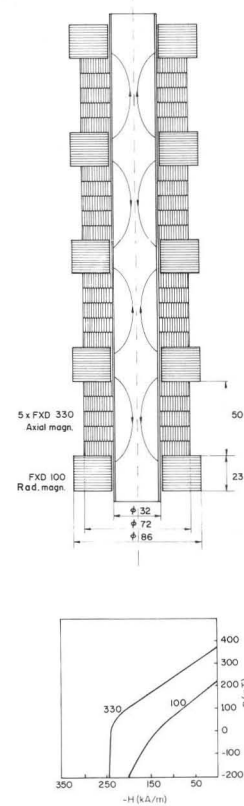


Fig. 4 : Four elements of the periodic structure. The large cores are made of isotropic Ferroxdure FXD100 and magnetised in radial direction. The FXD330 is an anisotropic material and magnetised axially. In adjacent elements the field is reversed. Below, the hysteresis curves of the two materials are given. The cores form a string around the vacuum tube. For a single element:  $\int B^2 dz = 155 \cdot 10^{-5} \text{ T}^2 \text{ m}$

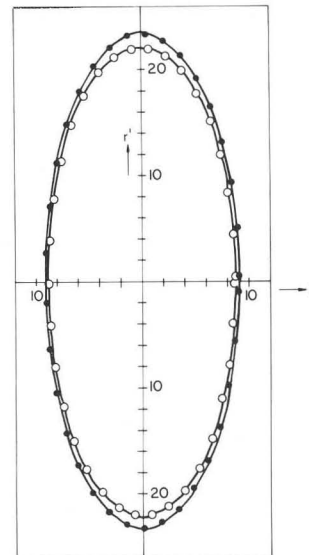


Fig. 5 : The distorted eigenellipse after two revolutions (trajectory periods). The open dots give the paraxial eigenellipse for a 600 mm mrad beam, the black dots the third revolution at the end of which the beam has travelled 7.5 m. The angle between two points is the step angle over one element.

distortion.

For a 1,2 mA 20 keV deuteron beam and 600 mm mrad the axis ratio  $\alpha$  will decrease with a factor of  $\sqrt{2}$ , due to space charge, if uncompensated, so the beam diameter would increase to 20 mm <sup>4)</sup>. An important number is also the distance covered by a particle moving along the axis and one moving along the outermost eigenellipse. The difference of both for our beam is 0.01 % <sup>4)</sup>.

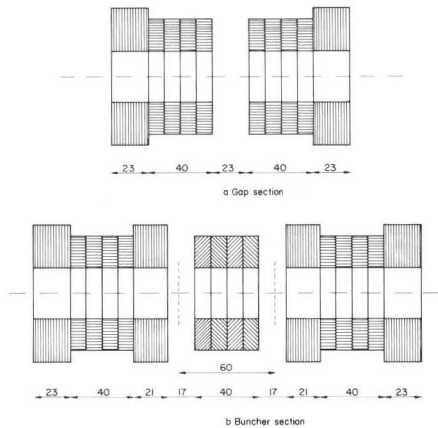


Fig. 6 : Fig. 6a shows the creation of a gap in the structure for mounting vacuum pumps etc. The radial ring has been removed and the length of each adjacent element is shortened by one axial ring.

Fig. 6b shows a solution for the integration of a buncher. 60 mm is the distance between the two buncher gaps. The four rings around the buncher channel could be replaced by a SmCo magnet with some advantages.

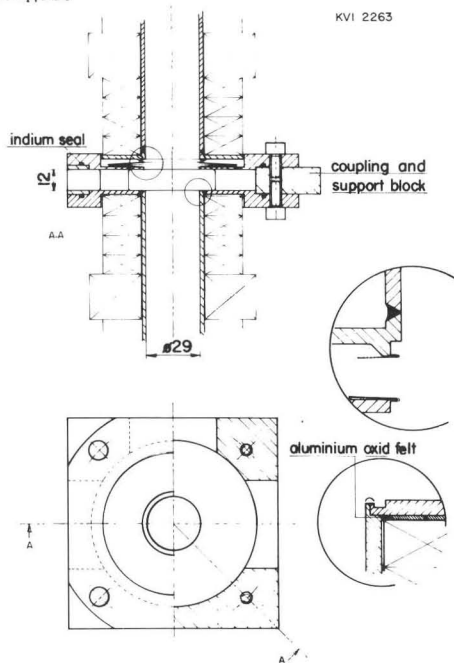


Fig. 7 : The lay out of the coupling between two sections of the periodic structure. The coupling block between the two flanges is fixed to the support. Indium wire is used for all sealings. The upper flange on the lower section has to be welded to the beampipe in the presence of the magnetized magnets.

The total length of the periodic structure is 7 m. To maintain a pressure of a few times  $10^{-7}$  mbar under beam load, calculations and test bench results <sup>7)</sup>

indicate that for the given beampipe diameter of 30 mm the distance between two vacuum pumps should not exceed 85 cm. The system will be divided in sections of 10 or 12 elements with a gap between. The gap is made by the removal of one radial ring and the influence in the beam is minimized by shorter sections of axial rings at both sides <sup>4)</sup>. Fig. 6 shows the solution for the gap and the buncher. Fig. 7 shows the lay-out of the coupling block for the vacuum pump, beam diagnostics, diaphragms etc. For the vacuum pumps triode ion getter pumps with a pumping speed of 30 l/s for Nitrogen and 7 l/s for Argon will be used. The pumping speed halfway every section will be about 12 l/sec for  $N_2$  and 6 l/sec for Ar. Provisions to apply a glow discharge over the whole length of the beampipe are foreseen.

An important point in the design of low energy ion transport lines is the excess desorption due to wall bombardment by ions. (The desorption rate for electron bombardment is one or two orders lower) <sup>5)</sup>. In the case of a well collimated beam the wall is hit mainly by ions produced by charge exchange. If we call  $\eta$  the number of desorbed atoms per primary ion and if we suppose for the moment that in a certain section  $\Delta\chi$  of the line the produced lower charge state ions also reach the wall there then the following formula can be derived:

$$n = \frac{A}{S - I\eta\sigma\Delta\chi}$$

$n$ =neutral gas density,  $A$ =normal wall degassing,  $S$ =effective pumping speed in  $\Delta\chi$ ,  $\sigma$ =total charge exchange cross-section,  $I$ =beam current in part/sec, For a beam of 100  $\mu A$   $4^+$  ions and  $\eta = 10$ ,  $\sigma = 5 \cdot 10^{-15} \text{ cm}^2$ ,  $\Delta\chi = 100 \text{ cm}$  we find:

$$I\eta\sigma\Delta\chi = 1000 \text{ cm}^3/\text{sec}$$

A few remarks: The given  $\eta$  holds for a clean wall under U.H.V. conditions <sup>5)</sup>. Organic contaminants may cause an increase of  $\eta$  up to one or two orders of magnitude. The lay out of the vacuum system should avoid this contamination <sup>7)</sup>. The assumption that the lower charge state ions reach the wall in the region where they are produced is not always true, but in long straight sections it does not matter which ions hit the wall. Beam ions in the outer edges of the phase space area which have had a charge exchange collision in a region before a lens system will reach the wall just in or after the next following lens. Ions which are more in the central part of the beam will travel to the end of a straight section and hit the wall e.g. just at the end of the axial hole in the cyclotron where the pumping speed is normally low. Here excessive beam loss or even instabilities may easily occur.

Test bench results show that an effective pretreatment is an argon glow discharge under a pressure between  $10^{-2}$  and  $10^{-1}$  m.bar. <sup>6)</sup>. This is especially effective in the case of Aluminium where a normal gas desorption of  $< 3 \cdot 10^{-10} \text{ Ncm}^3/\text{s}$  is obtained after the application of the glow discharge <sup>7)</sup>. This persists when the line is vented and shortly exposed to room conditions. To avoid organic contamination using turbo molecular pumps special care is needed in the starting up and shut down procedure <sup>7)</sup>.

If the beam is matched to the periodic structure the axis ratio of the phase space area depends on the energy. The acceptance of the cyclotron centre in constant orbit mode is more or less independent of energy. Therefore two cylindrical lenses are planned between the end of the periodic structure in the axial hole and the transition lens formed by the main magnet field at the end of the hole as shown in fig. 8. The phase space areas for a 600 mm mrad matched beam for two energies are shown too. Both magnetic lenses use the iron of the pole as return yoke. One side of the

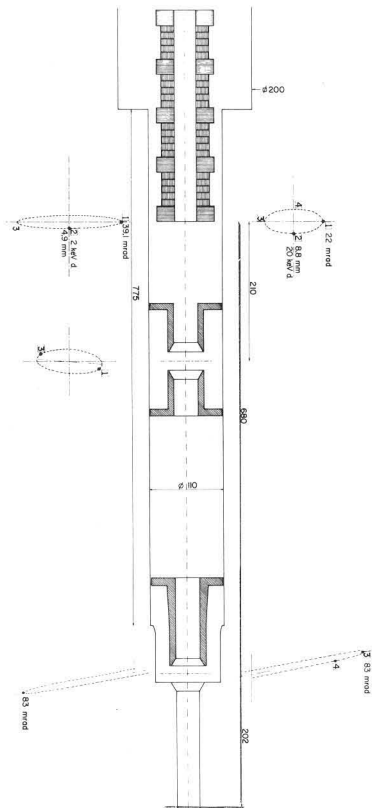


Fig. 8 : The end of the periodic system in the axial hole of the cyclotron magnet and the two lenses to match the beam to the cyclotron centre. The strong lens at the transition from the 34 mm hole into the main field of the cyclotron magnet gap is 20 cm from the last matching lens. This lens uses the cyclotron pole as one gap side and return yoke. The phase space ellipses are given for 20 keV and 2 keV deuterons as they leave the periodic system and the matching lenses.

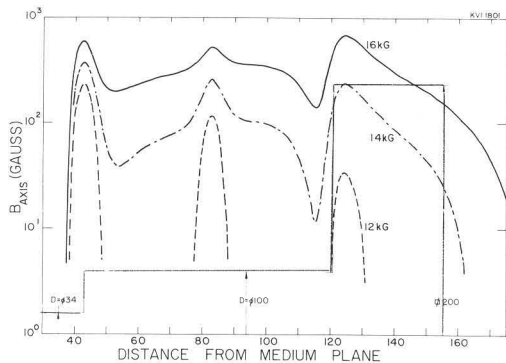


Fig. 9 : The measured stray field distribution in the axial hole for different main field strengths. The max. stray field at 16 kG is 600 G.

gap of the last lens is also formed by the pole iron, to make the distance to the transition lens as short as possible. At this location the pole is not saturated. A top field strength of 0.76 T is needed to focus the beam just before the transition lens. The iron of the two lenses is shaped to minimize the aberrations for a 600 mm mrad beam. Between the two lenses a titanium sublimation pump will be installed, which has to be designed especially for this system.

Two double gap bunchers are planned. One will be integrated in the periodic structure, fig. 6, and situated just outside the cyclotron yoke. The distance

to the centre is about 2.6 m. The second one will be situated between the end of the focussing structure and the first lens in the axial hole. The reason for using two bunchers is mainly to save RF energy. The power will be delivered by two 100W broadband transistor amplifiers matched to  $50 \Omega$ . The buncher voltage of 400 V (p-p) max. is realized by a broadband 2x step up transformer close to the buncher. It is intended to feed both bunchers with a linear triangular voltage. Another advantage of two bunchers is that the requirements on the triangle shape are smaller than in the case of one buncher. The phase of the voltage for the second buncher is not critical.

At the entrance of the periodic system in the ion source room again two cylindrical magnetic lenses of the same design as in the axial hole will be used to match the beam from the horizontal line (constant geometry) to the periodic structure. Two sets of two stepping motor beam scanners with centre of mass calculation<sup>8)</sup> are planned to control the shape and alignment of the beam.

In the axial hole the magnetic stray field, illustrated in fig. 9, will be compensated by coil sections as far as needed. Due to the absence of quadrupole lenses and the fact that the beam axis coincides with the cyclotron axis this compensation is not critical.

Central region design. - Since the bore in the cyclotron yoke to be used for axial injection coincides with the axis of the cyclotron poles over its entire length, an axially injected beam will initially be off-centred after inflection into the median plane. It is not feasible to adjust the injection energy of the injected beam for obtaining a centred beam since there are many other factors influencing the choice of this parameter. We decided to use a hyperboloidal inflector because of its superior optical properties<sup>9)</sup>. The maximum injection energy has been fixed at 20 kV, resulting in an initially off-centred beam.

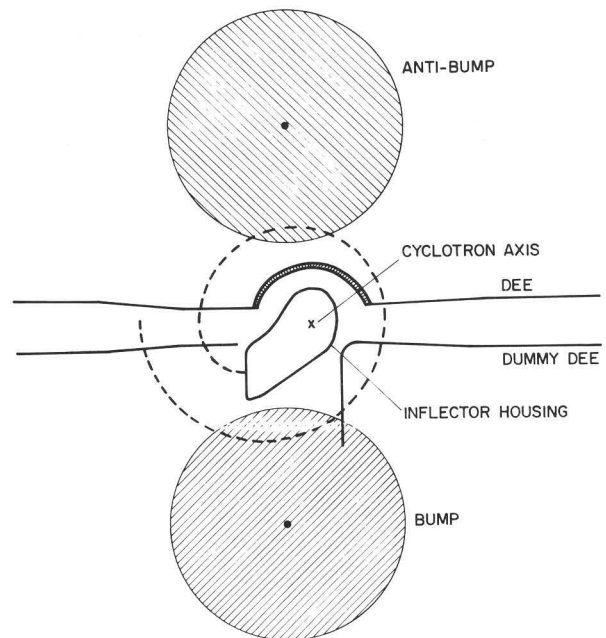


Fig. 10 : The layout of the central region for an axially injected beam. The radially inserted inflector can be replaced by an internal ion source.

Calculations have shown that it is not advisable to use an electrostatic device for correcting the centring

error (KVI Annual Report 1980, p.132). The centring problem may be solved, however, by using additional harmonics in the magnetic field for shifting the orbit centre towards the cyclotron centre during the first revolutions. These additional magnetic fields are produced by so-called bump and antibump coils, which will be mounted above and below the median plane against the RF liner. Fig. 10 shows the layout of the central region. The inflector is rotated in such a way, that the error in the orbit centre is along the accelerating gap. Centring may be obtained by using the bump or the antibump field or both. The last alternative does not disturb the isochronous field and is therefore to be preferred. The spatial size of the bumps is 10 cm FWHM, the maximum fields are 14 mT.

Extensive numerical orbit calculations have been performed. The field maps of the electric potential are obtained with the program RELAX-3D, developed at TRIUMF. The orbit integrations have been done with the program TRIWHEEL.

Fig. 11 shows the position of the orbit centers after 15 revolutions for an injected beam with an initial emittance of 800 mm.mrad as a function of the central position phase  $^{10}$ ). Therefore the areas in fig. 11 are areas of constant energy. In this case the bump-antibump combination is used in the fundamental mode of acceleration. Fig. 11 applies to the azimuth where the most recent acceleration has moved the instantaneous orbit centre to the left. It is therefore seen that the beam is well-centred on leaving the central region.

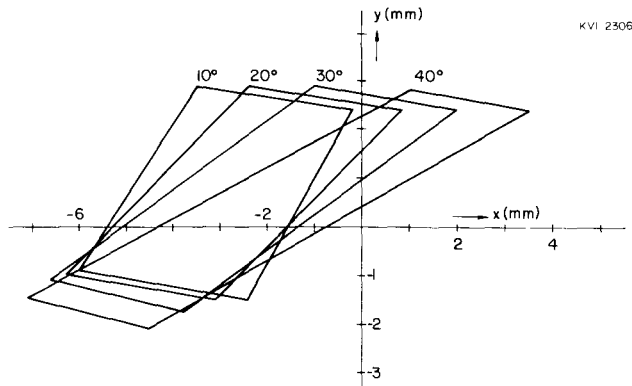


Fig. 11 : The radial emittance of an initially excentric beam after 15 revolutions in a magnetic field with the bump-antibump combination.

In order to obtain an estimate of the influence of the bump fields on radial beam quality, similar calculations have been performed for the hypothetical case of an initially centred beam without using bump

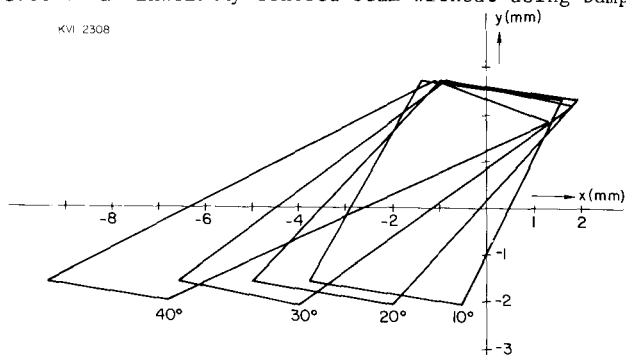


Fig. 12 : The radial emittance after 15 revolutions for the hypothetical case that the beam is centred from the beginning.

fields. The resulting radial phase space after 15 revolutions is shown in fig. 12. This figure shows that the bump does not influence the shape of the beam emittance. The influence of the CP phase on the emittance is, however, different for the two cases. In both cases, particles accelerated near the top of the RF wave make a larger jump during the first gap crossing than particles accelerated far from the RF maximum. These last particles, however, spend more time in the region occupied by the bump field, which slightly overcompensates the effect of the first gap crossing.

When the influence of the RF voltage on beam centring is investigated, a marked advantage for using the field bump appears. Fig. 13 shows the position of the orbit centers after 15 revolutions with a field bump and using a Dee voltage which is 50% larger than nominal. In fig. 14 a similar plot is given for the (hypothetical) initially centred beam. In both cases

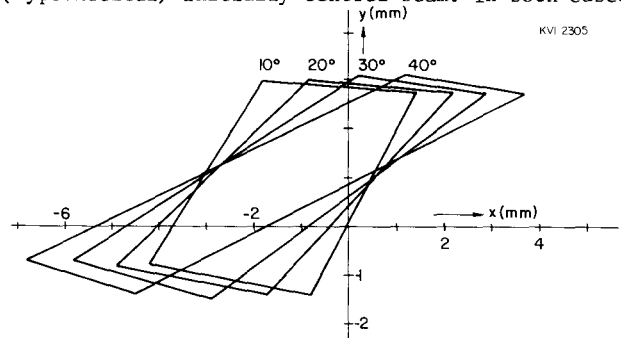


Fig.13 : The radial emittance of an initially excentric beam with the a Dee voltage which is 50% higher than nominal (after 15 revolutions).

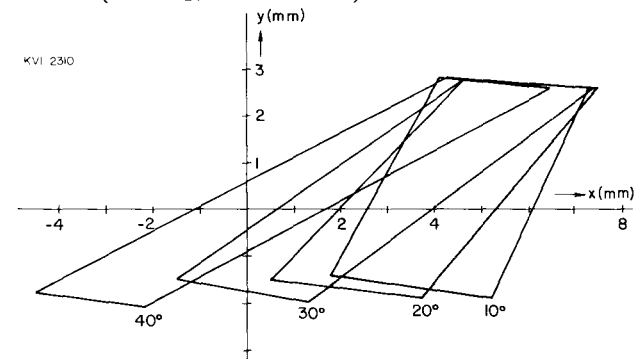


Fig.14 : The radial emittance for the hypothetical case that the beam is centred from the beginning. The Dee voltage is 50% higher than nominal (again after 15 revolutions).

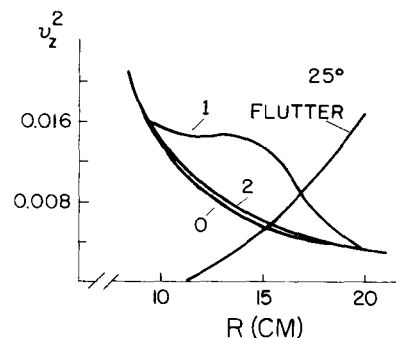


Fig. 15 : The vertical oscillation frequency as a function of radius. 0) without influence of the field bump, 1) with one single bump, and 2) the bump-antibump combination.

272 W.K. van Asselt et al.

the jump of the orbit centers at the first gap crossing is much larger than in the case of nominal Dee voltage, but the beam has made less revolutions in the bump-antibump, its influence therefore has decreased. Without a bump there is no compensation and the orbit centers of all particles are therefore shifted approximately 5 mm when compared to fig. 12.

The vertical particle motion may be investigated by determining the axial oscillation frequency  $\nu_z$ . Fig. 15 shows  $\nu_z^2$  as a function of radius. Due to the extra alternating gradient with the bump-antibump combination there is a slight increase in the axial oscillation frequency. When only one bump is used,  $\nu_z$  is significantly larger, resulting in a larger vertical acceptance. This is a result of the decrease of the field with radius in the region where  $\nu_z$  is minimal.

Shielding of the cyclotron stray field. - In the ion source room, which is on top of the cyclotron cave the stray field of the cyclotron adds up to +8.5 G to the existing field of -2.5 G. The vertical beam line connecting the ion source room with the cyclotron centre is basically insensitive to the stray field, but where it passes the roof the transverse components are rather high and possibly not axially symmetric. Further more there is the influence of a crane, which is not always in the same position.

For 20 keV  $d : B_p = 2.88 \times 10^{-2} Tm$  so in the horizontal beam line a field of 8.5 G over 5 m would give a deflection of 37 cm. Thus shielding of the stray field is rather essential.

Fig. 16 shows the proposed array of shielding plates on top of the cyclotron. The length and position of the plates has been estimated on the bases of field measurements 10 cm above the cyclotron yoke. Snell's law and saturation criteria are used to determine the shape and thickness. The flux density in the two lower plates will not exceed 1.5 T, in the upper one it is below 1 T. The shielding factor is expected to be about 10.

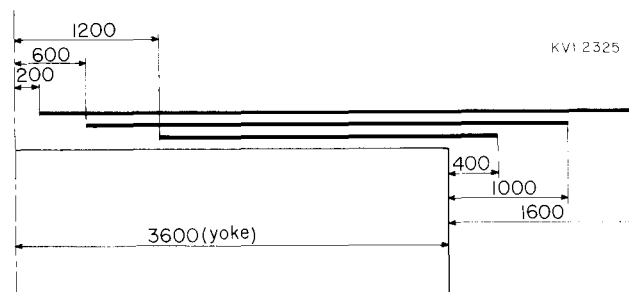


Fig. 16 : The magnetic shielding on top of the cyclotron. The three armco iron plates are of different length and cover the diameter of the coils. The thickness is 15 mm. The arrangement is symmetrical with respect to the cyclotron axis (most left).

#### References.

1. O.C. Dermois, A.G. Drentje, H.W. Schreuder, IEEE NS-26 (1979) 1992
2. R. Geller, *ibid.*, 2120;
3. Nucl. Instr. and Meth. 178 (1980) 305
4. O.C. Dermois. Proc. 5th Int. Cycl. Conf., Butterworths(1969), 620
5. O.C. Dermois. A periodic focussing structure for the transport of low energy ions. To be published in Nucl. Instr. and Meth.
6. M.H. Ackard et al. Vacuum, 29 (1979) 53
7. R.P. Govier, G.M. McGrachen Jounal Vac. Sc. Techn., Vol.7, no.5, page 552.
8. P.W. Schmidt et al. Vacuum test bench for the axial injection. K.V.I. report (in Dutch).
9. R.J. Vader, O.C. Dermois. Nucl. Instr. and Meth. 144 (1977) 423
10. R.W. Müller, Nucl. Instr. and Meth. 54 (1967) 29
11. W.M. Schulte, H.L. Hagedoorn, Nucl. Instr. and Meth. 171 (1980) 409

#### " DISCUSSION "

M. ZACH : Periodic structures of this type have been used for travelling wave tubes and later abandoned. One of the reasons was the low thermal stability of baryum ferrites. Could you comment on that ?

O.C. DERMOIS : I know about the use of ferrites in travelling wave tubes. At room temperature, we did not find much variation in measured field strength over a long period of time and having done numerous measurements. This within the accuracy of the measurements being a few percent. The requirements on the field stability are not large for this application.

M.K. CRADDOCK : What is the time scale for this project ?

O.C. DERMOIS : A shutdown of the cyclotron for 3 to 5 months is foreseen at the end of 1982 in order to make the changes in the axial hole and to build in the new centre.

M. REISER : With the use of permanent magnets in the periodic channel, you cannot vary the magnetic field. Do you have any problems in the transport of various ion species and energies due to this lack of field variation ?

O.C. DERMOIS : The point is partly treated in the article. Calculations on emittance matching from the horizontal line have shown that practically the matching should be rather easy using only the two cylindrical matching lenses and check the right conditions with the beam scanners. In fact, one has to adjust only these two lenses as function of energy (and space charge) in a well defined way.